Transient Kinetic Studies on the Interaction of Ras and the Ras-Binding Domain of c-Raf-1 Reveal Rapid Equilibration of the Complex[†]

Jens R. Sydor,[‡] Martin Engelhard,[‡] Alfred Wittinghofer,[§] Roger S. Goody,[‡] and Christian Herrmann*[,§]

Abteilung Physikalische Biochemie and Abteilung Strukturelle Biologie, Max-Planck-Institut für Molekulare Physiologie, Postfach 102664, 44026 Dortmund, Germany

Received April 6, 1998; Revised Manuscript Received July 27, 1998

ABSTRACT: Transient kinetic methods have been used to analyze the interaction between the Ras-binding domain (RBD) of c-Raf-1 and a complex of H-Ras and a GTP analogue. The results obtained show that the binding is a two-step process, with an initial rapid equilibrium step being followed by an isomerization reaction occurring at several hundred per second. The reversal of this step determines the rate constant for dissociation, which is on the order of 10 s^{-1}. The lifetime of the complex is therefore on the order of 50−100 ms, which is much shorter than the lifetime of GTP at the active site of H-Ras as determined by the intrinsic GTPase reaction. This suggests that multiple interactions of a single activated Ras molecule and Raf can occur, the number being limited by the competing interaction with GAP. The GDP complex of H-Ras binds more than 2 orders of magnitude more weakly than the GTP−analogue complex, mainly due to a significant weakening of the initial binding equilibrium reaction in the GDP state, thereby avoiding even short-lived recruitment of Raf to the plasma membrane by the inactive Ras form.

Raf (c-Raf-1) is a member of the serine/threonine kinase family and plays an important role in intracellular signal transduction. It is a soluble protein which is recruited to the plasma membrane by interaction with lipid-anchored Ras, this process resulting in activation or channeling of its kinase activity (*1*, *2*). Raf is thus regarded as a Ras effector. A region of the Raf protein (residues 51−131) has been identified as being responsible for the interaction with Ras, and this region is termed RBD[1] (Ras-binding domain) (*3*). The structure of RBD in complex with the Ras-like protein Rap1A in the GTP analogue-bound form has been determined (*4*), as has the affinity of the interaction of Ras with RBD (*5*). To understand the dynamics of signal transduction processes involving the Ras−Raf interaction, we need to have information not only on the affinity between the two proteins and on the manner in which this is dependent on the state of the guanosine nucleotide at the active site of Ras but also on the kinetics of these processes. Thus, for a given affinity between the two proteins, the rate of dissociation could differ by several orders of magnitude, thus determining whether Ras−GTP bound to Raf can only be converted to the inactive GDP form at the rate of the intrinsic GTPase reaction or whether multiple dissociation−association cycles can occur with the consequence being that proteins with GAP activity (*6*), which cannot exert their influence on the Ras−Raf complex (*7*−*10*), can potentially stimulate GTP hydrolysis. Previous evidence suggested that Raf can dissociate relatively rapidly from Ras, and a lower limit of 1 min^{-1} was placed on this rate constant (*11*).

Here we present transient kinetic data which show that the RBD fragment of Raf is indeed in relatively rapid equilibrium with its form bound to Ras−GTP, suggesting that multiple interactions of Ras−GTP and Raf can occur during the lifetime of the bound GTP, and that the exact number of interactions will depend on the relative effective concentrations of GAPs and Raf. The length of time that a Raf molecule spends bound to Ras−GTP before dissociation occurs is approximately 100 ms.

MATERIALS AND METHODS

Cloning, Expression, and Purification of the His-Tagged RBD Proteins. The cDNA of the Ras-binding domain corresponding to amino acid residues 50−132 with an additional His tag at the C terminus was cloned into a pET-19b vector. The plasmid was transformed into *Escherichia coli* BL21(DE3) cells for protein expression. BL21(DE3) cells contain a chromosomal copy of the T7 RNA polymerase gene under the control of the IPTG-inducible *lacUV5* promoter. Expression was induced by 1 mM IPTG. Three hours after induction, the cells were harvested by centrifugation and stored frozen at −80 °C.

For RBD/H purification, the frozen cell pellet was resuspended in buffer A [300 mM NaCl, 50 mM phosphate, and 5 mM imidazole (pH 8)] containing 0.05 μM aprotinin, 1 μM leupeptin, und 1 μM pepstatin as protease inhibitors.

[†] This work was supported by a grant from the Deutsche Forschungsgemeinschaft to C.H.

* To whom correspondence should be addressed. Telephone: +49 231 1206 351. Fax: +49 231 1206 230. E-mail: christian.herrmann@mpi-dortmund.mpg.de.

[‡] Abteilung Physikalische Biochemie.

[§] Abteilung Strukturelle Biologie.

[1] Abbreviations: GAP, GTPase activating protein; GDI, guanine nucleotide dissociation inhibition; L91W, mutant with leucine at position 91 replaced by tryptophan (other mutations are abbreviated correspondingly); GppNHp, guanyl-5′-yl imidodiphosphate, a nonhydrolyzable GTP analogue; IPTG, isopropyl β-D-thiogalactoside; mant, 2′,3′-(*N*-methylanthraniloyl), a fluorophor attached at the 2′- or 3′-position to the nucleotide; RBD, Ras binding domain of the human c-Raf-1 protein kinase comprising amino acids 51−131; RBD/H, RBD containing a C-terminal His tag.

S0006-2960(98)00764-8 CCC: $15.00
Published on Web 09/18/1998

After lysis of the cells in a microfluidizer (Microfluidizer M-110S, Microfluidics Corp., Newton, MA) at a final pressure of 1000 bar, and centrifugation, the cytoplasmic fraction was loaded onto a Ni^{2+}-NTA−agarose column. After washing with buffer A, the RBD was eluted by increasing the imidazole concentration to 250 mM. The combined RBD fractions were dialyzed against 100 mM NaCl, 50 mM Tris-HCl, and 5 mM $MgCl_2$ (pH 7.4), concentrated to ca. 1 mM with centrifugal concentrators (Filtron Technology Corp., Northborough, MA), shock-frozen in liquid nitrogen, and stored at −80 °C.

Site-directed mutagenesis by the overlap extension method (*12*) was used for the mutation of RBD at positions 91 and 114, and the products RBD L91W and RBD W114Y were verified by DNA sequencing.

Preparation of H-Ras and RBD. H-Ras and RBD were prepared as previously described (*5*, *13*). The Y32W mutant of Ras was prepared as described previously (*14*). Loading Ras with mantGppNHp or mantGDP was performed according to ref *15*.

Stopped-Flow Measurements. Stopped-flow measurements of the Ras−RBD interaction were carried out with a Hi-Tech Scientific SF-61 Single Mixing Stopped-Flow System, a SF-61MX Multi Mixing Stopped-Flow System, and an Applied Photophysics SX.17MV system. Excitation wavelengths were 289 nm for Trp excitation and 366 nm for excitation of the mant group fluorescence. Emitted light was monitored through filters with cutoff wavelengths of 320 and 389 nm, respectively. All measurements were taken in 100 mM NaCl, 50 mM Tris-HCl, and 5 mM $MgCl_2$ (pH 7.4). Data collection and primary analysis of rate constants were performed with the packages from High Tech Scientific or Applied Photophysics, while secondary analysis was performed with the program Grafit 3.0 (Erithacus software). Numerical simulation and fitting to a kinetic model was performed using the program Scientist (MicroMath). For the simultaneous fit to two data sets at different concentrations for the association of Ras−mantGppNHp and RBD L91W/H (Figure 5), the following model file was used for Scientist:

```
// Reversible second order reaction
IndVars: t
DepVars:A, B, C, A1, B1, C1, F, F1
Params: k1, k2, Ya, Yc
A'=-k1*A*B+k2*C
B'=-k1*A*B+k2*C
C'=k1*A*B-k2*C
F=A*Ya+C*Yc
A1'=-k1*A1*B1+k2*C1
B1'=-k1*A1*B1+k2*C1
C1'=k1*A1*B1-k2*C1
F1=A1*Ya+C1*Yc
//Parameter values
k1=10
k2=1
Ya=2.0
Yc=1.7
//Initial conditions
t=0.000
A=0.5
B=1
C=0
A1=0.5
B1=2
C1=0
***
```

A and A1 are the concentrations of Ras·mantGppNHp in the two experiments, B and B1 the concentrations of RBD L91W/H, and C and C1 the concentrations of the binary complexes. F and F1 are the observed fluorescence signals (photomultiplier output in volts), k1 and k2 the rate constants for the forward and reverse reactions, and Ya and Yc the fluorescence yields of Ras·mantGppNHp and its complex with RBD, respectively. A′, B′, etc., stand for d*A*/d*t*, d*B*/d*t*, etc. The units of concentration are μM, those of k1 μM^{-1} s^{-1}, and those of k2 s^{-1}. The units of Ya and Yc are V μM^{-1}. All four parameters were allowed to vary from the indicated starting values during the fit procedure. In the example shown, the same time base was used for each experiment, which allowed use of a common time base for the fits, with separate columns for F and F1 in the Scientist spreadsheet. In cases where different time bases are used, they are entered sequentially in the time column (t), and F, F1, etc., are in separate columns and appropriately displaced vertically.

RESULTS AND DISCUSSION

Earlier attempts to detect a change in fluorescence properties of the fluorescent guanosine derivative mantGppNHp at the active site of Ras on interaction of the complex with RBD suggested that no or only a very small change occurred, which was not sufficient for equilibrium titrations at the low concentrations of proteins needed because of their relatively high affinity (*5*). However, in stopped-flow experiments, a signal which was quite adequate for transient kinetic investigations at concentrations of Ras·mantGppNHp of ca. 0.5 μM was seen, and an example of the time course observed on mixing this complex with RBD is shown in Figure 1a. There is a drop in fluorescence on formation of the ternary complex, and the rate of the transient seen increased with increasing RBD concentrations. When the RBD concentration was high enough for pseudo-first-order conditions to pertain, the transient could be well fitted with a single-exponential term, and Figure 1b shows the concentration dependence of the fitted first-order rate constant. It can be seen that the dependence is linear at this temperature (25 °C) up to at least 750 s^{-1}, as would be expected for a simple second-order association reaction. The slope of the straight line through the points gives the apparent association rate constant, k_{ass}, and this is estimated to be 4.5×10^7 M^{-1} s^{-1}. The intercept of the straight line with the *y*-axis should give the dissociation rate constant, k_{diss}, but this cannot be reliably distinguished from zero with the data obtained. It should be noted that there will be a significant error on the points at low concentrations, since true pseudo-first-order conditions did not prevail, so that the intercept would not be reliable even if seen to be finite but small. k_{diss} was therefore measured directly as shown in Figure 2 by displacement of Ras·mantGppNHp from its complex with RBD by an excess of unlabeled Ras·GppNHp. The value obtained (7.4 s^{-1}) together with the association rate constant allowed a value of 160 nM for the K_d value for the interaction to be calculated. This is in good agreement with the K_d value of 130 nM obtained by the GDI method in the same buffer (*16*).

Although amplitude measurements with the small signals obtained were not very reliable, there was a tendency for the fluorescence change seen in the association transients to

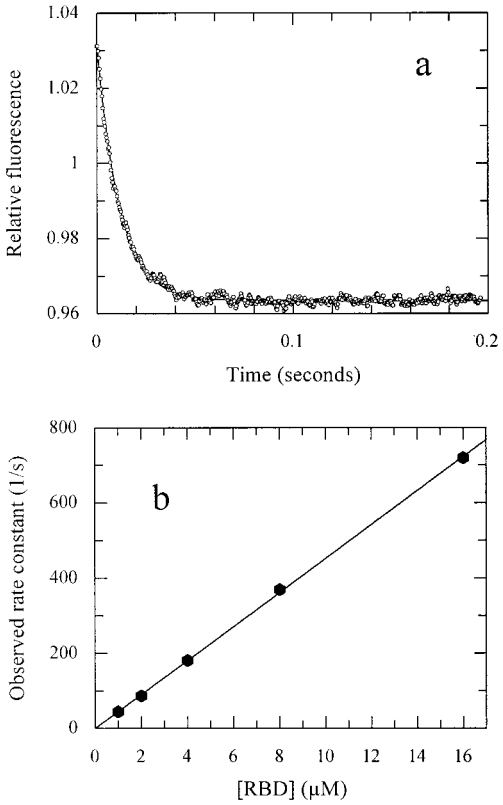

FIGURE 1: (a) Fluorescence transient observed on rapid mixing of Ras·mantGppNHp (0.5 μM) with RBD (2 μM) at 25 °C. The excitation wavelength was 366 nm with detection through a 389 nm cutoff filter. The fitted curve corresponds to a pseudo-first-order rate constant of 86 s^{-1}. (b) Plot showing the dependence of the pseudo-first-order rate constant obtained from experiments of the type shown in panel a on the RBD concentration. The slope of the fitted straight line corresponds to an apparent second-order rate constant of 4.5×10^7 M^{-1} s^{-1}.

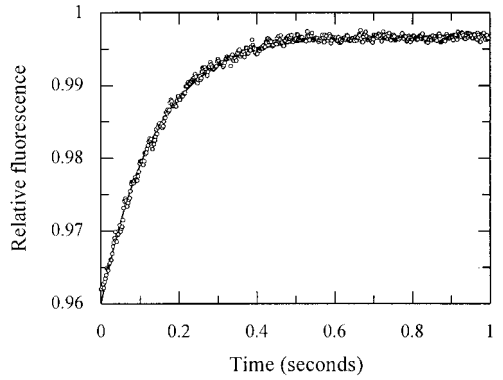

FIGURE 2: Dissociation of Ras·mantGppNHp (0.5 μM) from its complex with RBD (0.5 μM) after rapid mixing with Ras·GppNHp (4 μM) monitored by fluorescence excitation and detected as in Figure 1. The fitted curve corresponds to a rate constant of 7.4 s^{-1}.

be somewhat larger than in dissociation transients. A possible reason for this, which would also help explain the difficulty of demonstrating a fluorescence change in equilibrium experiments, would be the occurrence of an initial rapid increase in fluorescence within the mixing dead time of the stopped-flow instrument (1 ms) in a two-step binding mechanism, with the observed decreasing transient reflecting the fluorescence change between the first and the second bound states. While this question can be dealt with in

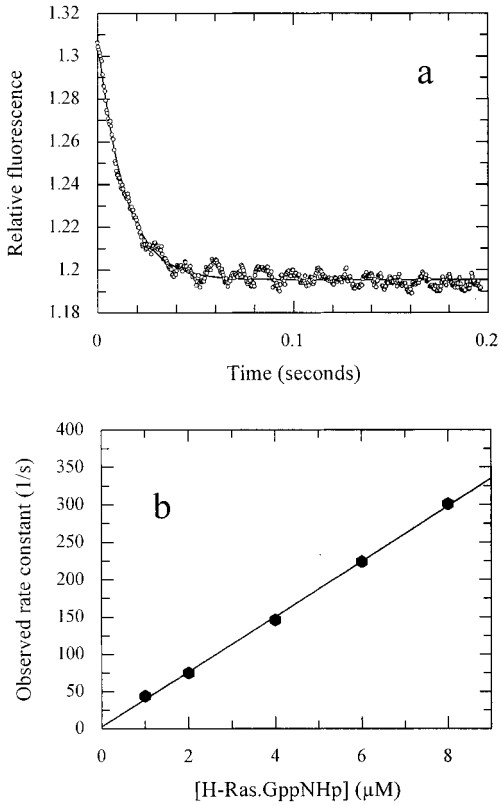

FIGURE 3: (a) Fluorescence transient observed on rapid mixing of Ras·GppNHp (2 μM) with RBD L91W/H (0.5 μM) at 25 °C. The excitation wavelength was 289 nm with detection through a 320 nm cutoff filter. The fitted curve corresponds to a pseudo-first-order rate constant of 75 s^{-1}. (b) Plot showing the dependence of the pseudo-first-order rate constant obtained from experiments of the type shown in panel a on the Ras·GppNHp concentration. The slope of the fitted straight line corresponds to an apparent second-order rate constant of 3.6×10^7 M^{-1} s^{-1}.

principle by measuring the baseline for the experiments by mixing Ras·mantGppNHp with buffer, in practice the variation of the total signal strength from run to run was too high in comparison with the small amplitudes being dealt with, so we cannot make a definite conclusion on this point.

Since it is possible, in principle, that the fluorescent label on the GTP analogue used for the studies described so far could have an influence on the interaction between Ras and RBD, we have also used tryptophan-containing mutants of RBD and Ras to study the Ras−RBD interaction. The site selected should meet two requirements. On one hand, the position should be close to the Ras−RBD interacting surface to provide information about the binding. On the other hand, the mutation should not impede the binding process. H-Ras has no tryptophan, and RBD has one tryptophan at position 114. When the structure of the Rap1A−RBD complex was taken into account (*4*), leucine 91 was replaced by tryptophan. When binding to Ras·GppNHp occurred, there was a useful drop in the fluorescence intensity of the L91W mutant (Figure 3a) without significantly disturbing the association−dissociation kinetics. As shown in Figure 3b, there was a linear dependence of the pseudo-first-order rate constant for the association reaction on the Ras concentration. The slope of the fitted straight line gave a value of 3.6×10^7 M^{-1} s^{-1} for the association rate constant, and a displacement experiment of the type described above led to a value of 14.0 s^{-1} for the dissociation rates. Thus, the

Table 1: Kinetic Parameters for the Interaction of Ras with RBD at 25 °C

reaction	k_{ass} (M^{-1} s^{-1})	k_{diss} (s^{-1})	K_d (μM)
RBD + Ras·mantGppNHp	4.5×10^7	7.4	0.16
RBD L91W/H + Ras·mantGppNHp	1.9×10^7	14.8	0.78
RBD/H + Ras·mantGppNHp	2.1×10^7	6.4	0.30
RBD L91W/H + Ras·GppNHp	3.6×10^7	14	0.38
RBD + Ras·mantGDP	1.1×10^6	36	32

binding kinetics were similar to those seen with the wild type RBD sequence using the fluorescently labeled nucleotide. In further experiments, it was shown that the polyhistidine C-terminal tail used for the L91W mutant did not have a significant effect on the association and dissociation kinetics of Ras·GppNHp and RBD. The results of these measurements at 25 °C are collated in Table 1.

Since the second-order rate constants for association measured in the experiments reported are somewhat lower than expected for a diffusion-controlled reaction, experiments were repeated at lower temperatures to look for signs of saturation of the observed pseudo-first-order rate constant of association at high concentrations, as would be expected for a two-step binding reaction. As shown in Figure 4, at 15 °C, the relationship between the observed rate constant and the RBD concentration is not linear but hyperbolic and could be fitted by a hyperbolic expression. This suggests that there are at least two steps in the binding interaction, and a likely mechanism is shown in Scheme 1.

Scheme 1

$$\text{RBD} + \text{Ras.mantGppNHp} \underset{k_{-1}}{\overset{k_{+1}}{\rightleftharpoons}} \text{RBD.Ras.mantGppNHp} \underset{k_{-2}}{\overset{k_{+2}}{\rightleftharpoons}} \text{RBD.Ras*.mantGppNHp}$$

According to this scheme, and assuming k_{-1} to be large compared to k_{+2}, and that the observed fluorescence change occurs in the second step, the observed pseudo-first-order rate constant in experiments of the type depicted in Figure 4 is given by the following expression:

$$k_{obs} = \frac{k_{+2}}{1 + 1/(K_1[\text{RBD}])} + k_{-2} \qquad (1)$$

In the fit to this equation shown in Figure 4, we have included the points at low (1 and 2 μM) RBD concentrations. But since these conditions were not properly pseudo-first-order, we analyzed the corresponding transients as second-order reactions. The derived value of the second-order rate constant was used to calculate the predicted pseudo-first-order rate constant which would be obtained using a concentration of Ras·mantGppNHp which was actually much lower than the 0.5 μM value used. While it is clear that this is not neccessarily a rigorously correct approach, these points have no effect on the estimation of the two parameters which can be estimated reliably from these data, i.e., the maximum rate constant for the fluorescence change and the apparent association constant (K_1) for the concentration dependence of the rate constant. The intercept on the *y*-axis was too small to allow its accurate estimation from this procedure. As described below and in Figure 5, we have

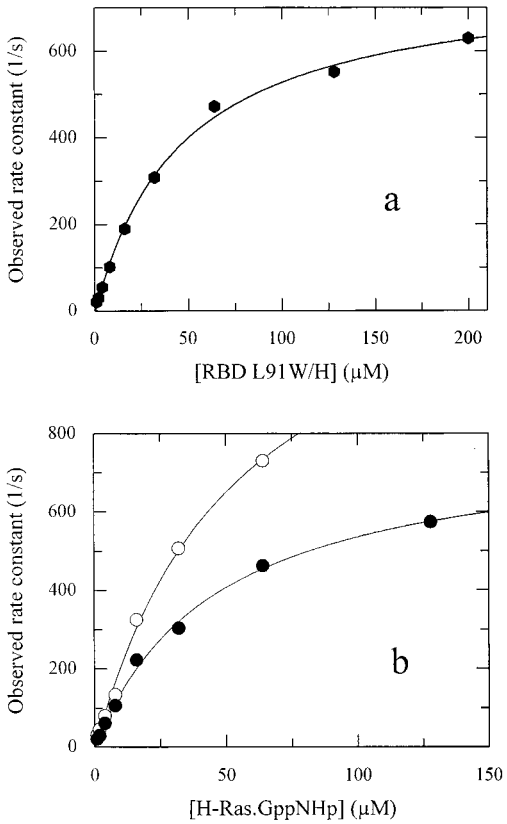

FIGURE 4: (a) Plot showing the dependence of the pseudo-first-order rate constant for association of Ras·mantGppNHp with RBD L91W/H on the concentration of the latter. Conditions were like those described in the legend of Figure 1 except that the temperature was 15 °C. The curve shows the result of fitting a hyperbolic function with a maximal rate constant of 778 s^{-1} and a value of 51 μM for $1/K_1$. The intercept with the *y*-axis could not be reliably distinguished from zero. The rate constant for dissociation was estimated directly from an experiment of the type shown in Figure 2 to be 8.7 s^{-1}. (b) Plot showing the dependence of the pseudo-first-order rate constant for association of Ras·GppNHp with RBD L91W/H on the concentration of the former. Conditions were like those described in the legend of Figure 3 except that the temperature was 10 (●) and 15 °C (○). A fit of a hyperbolic function to the data yielded maximal rate constants of 780 and 1380 s^{-1}, respectively, and $1/K_1$ values of 46 and 54 μM, respectively.

analyzed the points at low concentrations in a different manner to obtain further parameters.

Figure 5 shows the results of simultaneously fitting fluorescence transients obtained at the two lowest concentrations of RBD L91W used in the experiment of Figure 4 (1 and 2 μM). The program Scientist was used to numerically simulate the time course of the association reaction and to fit the same set of rate constants and fluorescence yields for both time courses. Since at the low concentrations used there is essentially no information in the data concerning the two-step binding (the protein concentrations are much too low for saturation effects to influence the data), the reaction mechanism was depicted as a simple one-step process in this case. The constants obtained (see the legend of Figure 5) agreed well with those obtained from the concentration dependence of the association reaction (Figure 4) and those from direct measurement of the dissociation reaction by displacement. The relatively large amount of information that can be derived from the two curves comes from the fact that the concentrations used are nonsaturating for the overall

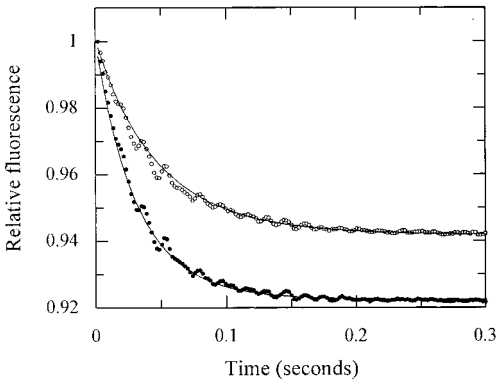

FIGURE 5: Result of simultaneously fitting the data points at low concentrations in Figure 4 using the program Scientist. The model used was one with a simple one-step association reaction; the differential equations describing this sytem were used to simulate the time course of the reaction by numerical integration, and constants were fitted to the data. The fit shown corresponds to values of 1.25×10^7 M^{-1} s^{-1} for the association rate constant and 7.1 s^{-1} for the dissociation rate constant. These agree well with those which can be calculated from the constants given in the legend of Figure 4 (effective association rate constant of 1.52×10^7 M^{-1} s^{-1} and dissociation rate constant of 8.7 s^{-1}).

reaction, as seen from the difference in amplitudes for the two traces.

The interpretation of the nonlinear dependence of the pseudo-first-order rate constant for the association of RBD and Ras·mantGppNHp given here is based on the assumption that the time-dependent signal seen arises from a drop in fluorescence associated with the second step in Scheme 1. As outlined above, the possibility that a fluorescence change in the opposite direction occurs in an initial rapid binding step cannot be excluded. The interpretation given here is, however, not affected by the possible occurrence of this change in fluorescence yield.

As has been discussed previously (*17*), data of the type obtained do not allow a distinction between the mechanism shown in Scheme 1 and that shown in Scheme 2, in which there is an isomerization of the Ras·mantGppNHp complex prior to formation of RBD·Ras·mantGppNHp.

Scheme 2

$$\text{RBD + Ras.mantGppNHp} \underset{k_{-1}}{\overset{k_{+1}}{\rightleftharpoons}} \text{RBD + Ras*.mantGppNHp} \underset{k_{-2}}{\overset{k_{+2}}{\rightleftharpoons}} \text{RBD.Ras*.mantGppNHp}$$

On the basis of this scheme, if we make the reasonable assumption that k_{-1} is much larger than k_{+1} (this must be true if the species predominantly populated in the absence of RBD is Ras·mantGppNHp) and also much larger than k_{-2} (this would correspond to the measured dissociation rate of ca. 7 s^{-1}), the apparent pseudo-first-order rate constant for the association reaction is given by the following expression:

$$k_{obs} = \frac{k_{+1}}{1 + k_{-1}/(k_{+2}[\text{RBD}])} + \frac{k_{-2}}{1 + k_{+2}[\text{RBD}]/k_{-1}} \quad (2)$$

Thus, increasing the concentration of RBD would lead to an approximately hyperbolic increase of the observed rate constant from k_{-2} at low concentrations to k_{+1}, the rate constant of the isomerization reaction, at saturating concentrations. The apparent K_d value from the hyperbolic fit would correspond to k_{-1}/k_{+2}, instead of k_{-1}/k_{+1} for the model in Scheme 1. It should be noted that in this case, the fluorescence change could occur in either the first step or the second, since both would lead to saturation binding kinetics.

Since the experiment described in Figure 4a cannot distinguish between the models of Schemes 1 and 2, an analogous experiment was performed which is shown in Figure 4b. Using the tryptophan fluorescence signal of the RBD L91W mutant, the kinetics of association with Ras·GppNHp were investigated. As shown in Figure 4b, there was a definite indication of saturation of the observed rate constant for association at 15 °C, despite the fact that the signal that is weaker and noisier than that from the mant group made the data less reliable. At 10 °C, saturation behavior was obvious, and the parameters obtained from the fits to these data agreed quite well with those of Figure 4a using Scheme 1 as a model. Perfect agreement is not expected, since in one case the nucleotide was GppNHp and in the other its fluorescently labeled derivative. The results shown in Figure 4b cannot be explained using the model of Scheme 2, since increasing the concentration of Ras·GppNHp would not lead to saturation behavior. An extended model, in which conformational changes of both Ras·GppNHp and RBD must occur before association, would lead to saturation behavior, but the maximal rate constant for binding would be different, in the general case, depending on which of the reactants is varied and which is held constant. In addition to this, there would be a departure from single-exponential transients in certain concentration ranges. A further problem with this model is that two energetically unfavorable isomerizations must occur before association, which must be overcome energetically by the protein−protein interaction, which would therefore have to be of much higher affinity than that which can be realized with a dissociation rate constant in this step of ca. 7−14 s^{-1}, as measured directly. This problem cannot be overcome by choosing the equilibrium constant for the isomerization reactions to be not too much smaller than unity, since this would lead to observable biphasic association transients. We therefore conclude that association of RBD and Ras·GppNHp (and by implication Ras·GTP) occurs via the mechanism shown in Scheme 1.

The association kinetics of Ras and RBD could also be monitored using the tryptophan-containing Ras mutant Y32W (*14*, *18*). To restrict the potential signal to the Ras protein, the tryptophan at position 114 in RBD was replaced by tyrosine. Interaction of Ras Y32W with RBD W114Y led to an increase of tryptophan fluorescence (Figure 6a), and the pseudo-first order rate constant for this process increased with increasing RBD concentrations. As described above for wild type Ras as a complex with mantGppNHp, the dependence was obviously nonlinear at temperatures below 25 °C, and Figure 6b shows the results obtained at three different temperatures. The data obtained show that the combination of the mutations introduced into the two proteins weakened the affinity considerably, and a major contribution to this comes from an increased dissociation rate in comparison with those of wild type proteins. Because of this, it is much easier to determine this dissociation rate constant from plots such as those shown in Figure 6b, and Table 2

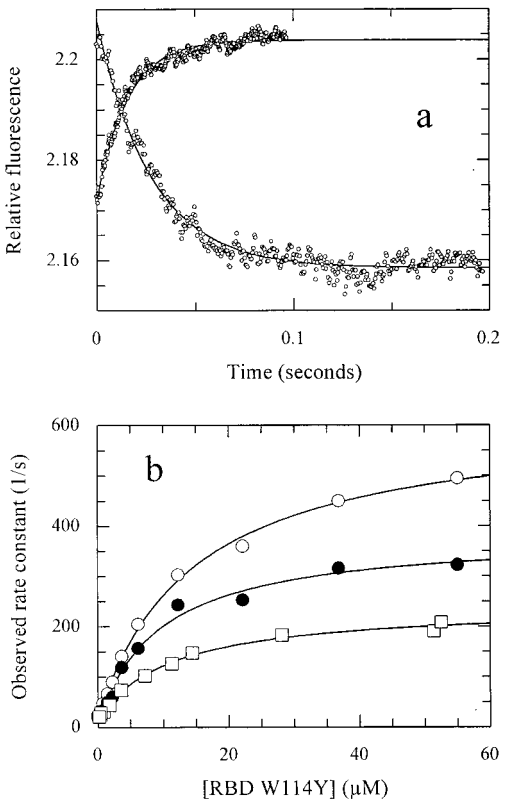

FIGURE 6: (a) Increasing fluorescence transient observed on rapid mixing of Ras Y32W·GppNHp (0.25 μM) with RBD W114Y (1.5 μM) and decreasing fluorescence transient observed for the dissociation of Ras Y32W·GppNHp (0.5 μM) and RBD W114Y (1.4 μM) by displacement with Ras·GppNHp (12 μM) at 25 °C. The excitation wavelength was 289 nm with detection through a 320 nm cutoff filter. The fitted curves correspond to a pseudo-first-order rate constant of 65 s^{-1} and to a dissociation rate constant of 36.5 s^{-1}. The larger amplitude seen in the dissociation compared to that in the association reaction suggests that a rapid fluorescence increase may occur within the dead time of the apparatus, but the accuracy of the data was not adequate to make a definitive decision on this point. (b) Plots showing the dependence of the pseudo-first-order rate constant on the RBD W114Y concentration obtained from experiments mixing Ras Y32W·GppNHp and RBD W114Y at 10, 15, and 20 °C (from bottom to top). Parameters obtained from fits according to eq 1 are listed in Table 2.

lists the values obtained for the equilibrium constant for the first (rapid) step, the forward rate constant of the second step, and the reverse rate constant for the second step obtained from measurement of the association kinetics. In addition, the value for k_{-2} determined from direct displacement reactions is included. As can be seen, there is reasonable agreement between the k_{-2} values determined by the two methods. The combined effects of the two mutations lead to a significant lowering of affinity, and comparison of the results in Tables 1 and 2 shows that this is mainly due to an increase in the dissociation rate constant.

The determination of the association and dissociation kinetics for the interaction between Ras Y32W and RBD W114Y at different temperatures allowed calculation of the effective activation energies of the overall association reaction and the dissociation process. These were found to have similar magnitudes (6.5 and 8.8 kcal/mol for the forward and reverse reactions, respectively), and these allowed estimation of their values and of affinities at temperatures other than those used experimentally. This was useful for

Table 2: Kinetic Parameters for the Interaction of Ras Y32W·GppNHp with RBD W114Y[a]

temp (°C)	$1/K_1$ (μM)	k_2 (s^{-1})	k_{ass} (μM^{-1} s^{-1})	k_{-2}[b] (s^{-1})	k_{-2}[c] (s^{-1})	K_d[d] (μM)
10	11	225	15	18	14	0.93
15	9.3	375	24	15	20	0.83
20	14.5	600	30	25	24	0.80
25	–	–	35	24	37	1.05
30	–	–	43	37	41	0.95
35	–	–	–	–	47	–

[a] K_1, k_2, and k_{-2} are as in Scheme 1. k_{ass} is the apparent second-order rate constant for the association reaction estimated from the approximately linear dependence of the observed rate constant on the RBD concentration at low concentrations compared with $1/K_1$. Comparison with the values calculated from K_1 and k_2 suggests that linear fitting to the low-concentration points results in an underestimate of this parameter, but we include the values of k_{ass} obtained by this procedure to allow comparison with the values obtained at higher temperatures, since under these conditions saturation of the observed rate constant could not be observed, thus precluding determination of K_1 and k_2. k_{-2} corresponds to k_{diss} in Table 1. [b] Determined from the intercept on the *y*-axis of plots as shown in Figure 6b. [c] Determined by displacement reactions as shown in Figure 6a. [d] Calculated from k_{ass} and the value of k_{-2} obtained by displacement reactions.

comparing the affinity between the two proteins derived from the association and dissociation rate constants with that measured by a different method, namely, the GDI method as reported previously (*5*). Using this method, which relies on quantitating the effect of protein−protein interaction on the dissociation rate constant of the nucleotide bound to Ras, high temperatures had to be used because otherwise the dissociation rates for practical measurements at lower temperatures are much too slow. The K_d value for the Ras Y32W·mantGppNHp−RBD W114Y interaction determined by this method at 35 °C was 0.8 μM (C. Herrmann, unpublished). Using the values for the effective association rate constant and the dissociation rate constant adjusted to 35 °C with the measured activation energies, a value of ca. 1 μM was obtained, in good agreement with the value obtained earlier.

Investigating the kinetics of interaction of RBD with the GDP-bound form of Ras was also of interest. This was done using Ras with mantGDP at the active site. As with mantGppNHp, there was a measurable fluorescence change on forming the complex with RBD, but the apparent association rate constant was much slower than for the mantGppNHp complex (ca. 1.1×10^6 M^{-1} s^{-1} at 25 °C, or a factor of ca. 40 lower than that for Ras·mantGppNHp), while the dissociation rate constant was considerably faster (36 s^{-1}; data not shown). Thus, the K_d (32 μM) was 200-fold higher than that for Ras·mantGppNHp as given in Table 1. The difference in the association rate constants of the GDP and GppNHp forms of Ras is considerably larger than that in the dissociation rate constants. In the case of GDP, as for GppNHp under the same conditions, a plot of the observed first-order rate constant for the association reaction against the RBD concentration was linear up to at least 200 s^{-1}. This suggests that k_{+2} in the mechanism of Scheme 1 is not significantly lower for Ras·GDP than for Ras·GppNHp so that the reduction in the apparent association rate must be due to a considerable weakening of the initial interaction (step 1 of Scheme 1) before the isomerization reaction takes place.

CONCLUSIONS

The results reported here define the kinetics of interaction between RBD and H-Ras with a guanosine triphosphate analogue at the active site. They show that when the two proteins interact, a relatively unstable complex is formed initially which then undergoes a conformational change occurring at a rate of several hundred per second to give a complex in which the affinity is 1−2 orders of magnitude higher than in the first bound state. This state can be equated structurally with the complex of Rap and RBD which was solved by X-ray diffraction (*4*), but we have no indication at present of how this differs from the first bound state. Thus, the second step in the binding mechanism might be a large conformational change, but could also be a much smaller local rearrangement after initial recognition and docking.

Whatever the nature of the processes occurring during binding, a knowledge of the rates of interconversion between the species is important for understanding the cell biological role of the interaction. Thus, depending on the lifetime of the Ras−Raf complex, the consequences of the interaction can be subtly but fundamentally different. If, for example, the lifetime were long compared with the GTP hydrolysis rate, each molecule of Ras·GTP which interacted with Raf would remain in the complex until GTP hydrolysis occurred to allow dissociation. Since the significance of the Ras−Raf interaction is probably recruitment of Raf to the vicinity of the plasma membrane of the cell, where Ras is located (*1*, *2*), this would mean that the "activating" interaction would also last this long. It is known that Ras cannot interact simultaneously with Raf and GAP (*7*−*10*), so that the lifetime of the species would be governed by the slow basal Ras GTPase reaction. This would not be logical if the cell biological result of the interaction really is a phosphorylation of Raf, since this process could presumably happen on a much faster time scale, and Raf must also presumably leave the vicinity of the membrane-bound Ras to interact with the next molecule in the signal transduction pathway. It is therefore consistent with these ideas that the lifetime of the Ras·RBD complex is relatively short according to the results presented here and in agreement with those reported earlier by Gorman et al. (*11*). The dissociation rate constant of the Ras·GTP·RBD complex is ca. 10 s^{-1} at 37 °C, meaning that after formation of the complex, its mean lifetime is ca. 50−100 ms.

Nevertheless, the mechanism of Raf activation by Ras is still a matter of considerable controversy (*19*). Although the primary role of Ras as a recruitment factor for Raf as evidenced by the Raf−Caax targeting experiments (*1*, *2*) is undisputed, the question of whether this recruitment is sufficient for activation with Ras acting as an allosteric regulator of Raf activity (*20*) or whether an additional event such as phosphorylation by a membrane-bound kinase (*21*−*25*) or a trans phosphorylation by dimerized Raf itself is responsible (*26*, *27*) has not been resolved. The results presented here can only elucidate the initial complex formation and not the whole activation of Raf by Ras and other factors. The lifetime of the RafRBD·Ras complex might be adequate on one hand for phosphorylation of Raf to occur and would have the advantage that the activated form of Raf does not stay bound to Ras for an unneccessarily long time, one of the consequences of this being that Ras·GTP is available for the downregulating effect of GAP after dissociation of Raf. The lifetime of the Ras·GTP complex would then be controlled by the effective GAP concentration and the competition of GAP and Raf for binding to Ras·GTP. However, for an allosteric type of activation of Raf by Ras, the lifetime of the complex might be too short. This could mean that other factors contribute to the tightness of the Ras−Raf complex, which are supplied by the plasma membrane and/or other domains of the Raf kinase. A contributing factor could be the cysteine-rich domain of Raf adjacent to the RBD, which has been suggested to contribute to the binding of Ras (*28*, *29*), possibly via the farnesyl group (*30*, *31*), and at the same time to the interaction with lipid components such as phosphatidylserine and phosphatidic acid (*32*).

The experiments reported on the interaction of the GDP-bound form of Ras confirm the much weaker binding of this form to RBD. On the basis of the two-step binding mechanism established in this work for the GppNHp complex, and on the basis of the knowledge of two-step mechanisms of binding of , for example, nucleotides to ATPases and GTPases, it was expected that the main difference in the kinetics of the interaction in the present case would be in k_{-2}, the rate constant of the rate-limiting step in the dissociation of the complex. However, in the present case, this effect was relatively small (a factor of ca. 5 between the two forms of Ras). The major effect appeared to be on the equilibrium constant of the initial weak binding reaction, suggesting that discrimination at this step is important. The cell biological advantage of this discrimination mechanism could be that even a transient retention of Raf in the region of the plasma membrane is avoided in the case of the Ras·GDP complex.

REFERENCES

1. Leevers, S. J., Paterson, H. F., and Marshall, C. J. (1994) *Nature 369*, 411−414.
2. Stokoe, D., Macdonald, S. G., Cadwallader, K., Symons, M., and Hancock, J. F. (1994) *Science 264*, 1463−1467.
3. Vojtek, A. B., Hollenberg, S. M., and Cooper, J. A. (1993) *Cell 74*, 205−214.
4. Nassar, N., Horn, G., Herrmann, C., Scherer, A., McCormick, F., and Wittinghofer, A. (1995) *Nature 375*, 554−560.
5. Herrmann, C., Martin, G. A., and Wittinghofer, A. (1995) *J. Biol. Chem. 270*, 2901−2095.
6. Boguski, M. S., and McCormick, F. (1993) *Nature 366*, 643−654.
7. Zhang, X.-f., Settleman, J., Kyriakis, J. M., Takeuchi-Suzuki, E., Elledge, S. J., Marshall, M. S., Bruder, J. T., Rapp, U. R., and Avruch, J. (1993) *Nature 364*, 308−313.
8. Warne, P. H., Rodriguez Viciana, P., and Downward, J. (1993) *Nature 364*, 352−355.
9. Scheffler, J. E., Waugh, D. S., Bekesi, E., Kiefer, S. E., LoSardo, J. E., Neri, A., Prinzo, K. M., Tsao, K.-L., Wegrzynski, B., Emerson, S. D., and Fry, D. C. (1994) *J. Biol. Chem. 269*, 22340−22346.
10. Herrmann, C., Horn, G., Spaargaren, M., and Wittinghofer, A. (1996) *J. Biol. Chem. 271*, 6794−6800.
11. Gorman, C., Skinner, R. H., Skelly, J. V., Neidle, S., and Lowe, P. N. (1996) *J. Biol. Chem. 271*, 6713−6719.
12. Ho, S. N., Hunt, H. D., Horton, R. M., Pullen, J. K., and Pease, L. R. (1989) *Gene 77*, 51−59.
13. Tucker, J., Sczakiel, G., Feuerstein, J., John, J., Goody, R. S., and Wittinghofer, A. (1986) *EMBO J. 5*, 1351−1358.
14. Rensland, H., John, J., Linke, R., Simon, I., Schlichting, I., Wittinghofer, A., and Goody, R. S. (1995) *Biochemistry 34*, 593−599.

15. Ahmadian, M. R., Hoffmann, U., Goody, R. S., and Wittinghofer, A. (1997) *Biochemistry 36*, 4535−4541.
16. Block, C., Janknecht, R., Herrmann, C., Nassar, N., and Wittinghofer, A. (1996) *Nat. Struct. Biol. 3*, 244−251.
17. Bagshaw, C. R., Eccleston, J. F., Eckstein, F., Goody, R. S., Gutfreund, H., and Trentham, D. R. (1974) *Biochem. J. 141*, 351−364.
18. Yamasaki, K., Shirouzu, M., Muto, Y., Fujita-Yoshigaki, J., Koide, H., Ito, Y., Kawai, G., Hattori, S., Yokoyama, S., Nishimura, S., and Miyazawa, T. (1994) *Biochemistry 33*, 65−73.
19. McCormick, F., and Wittinghofer, A. (1996) *Curr. Opin. Biotechnol. 7*, 449−456.
20. Stokoe, D., and McCormick, F. (1997) *EMBO J. 16*, 2384−2396.
21. Williams, N. G., Roberts, T. M., and Li, P. (1992) *Proc. Natl. Acad. Sci. U.S.A. 89*, 2922−2926.
22. Fabian, J. R., Daar, I. O., and Morrison, D. K. (1993) *Mol. Cell. Biol. 13*, 7170−7179.
23. Marais, R., Light, Y., Paterson, H. F., and Marshall, C. J. (1995) *EMBO J. 14*, 3136−3145.
24. Morrison, D. K., Heidecker, G., Rapp, U. R., and Copeland, T. D. (1993) *J. Biol. Chem. 268*, 17309−17316.
25. Kolch, W., Heidecker, G., Kochs, G., Hummel, R., Vahidi, H., Mischak, H., Finkenzeller, G., Marmé, D., and Rapp, U. R. (1993) *Nature 364*, 249−252.
26. Farrar, M. A., Alberola-Ila, J., and Perlmutter, R. M. (1996) *Nature 383*, 178−181.
27. Luo, Z., Tzivion, G., Belshaw, P. J., Vavvas, D., Marshall, M., and Avruch, J. (1996) *Nature 383*, 181−185.
28. Brtva, T. R., Drugan, J. K., Ghosh, S., Terrell, R. S., Campbell-Burk, S., Bell, R., and Der, C. J. (1995) *J. Biol. Chem. 270*, 9809−9812.
29. Drugan, J. K., Khosravi-Far, R., White, M. A., Der, C. J., Sung, Y.-J., Hwang, Y.-W., and Campbell, S. L. (1996) *J. Biol. Chem. 271*, 233−237.
30. Hu, C.-D., Kariya, K.-i., Tamada, M., Akasaka, K., Shirouzu, M., Yokoyama, S., and Kataoka, T. (1995) *J. Biol. Chem. 270*, 30274−30277.
31. Luo, Z., Diaz, B., Marshall, M. S., and Avruch, J. (1997) *Mol. Cell. Biol. 17*, 46−53.
32. Gosh, S., Strum, J. C., Sciorra, V. A., Daniel, L., and Bell, R. M. (1996) *J. Biol. Chem. 271*, 8472−8480.

BI980764F